



This is the author's version published as:

Jansen, Janine and Melchels, Ferry P.W. and Grijpma, Dirk W. and Feijen, Jan (2009) *Fumaric acid monoethyl ester-functionalized poly(D,L-Lactide)/N-vinyl-2-pyrrolidone Resins for the preparation of tissue engineering scaffolds by stereolithography.* Biomacromolecules, 10(2). pp. 214-220.

Copyright 2009 American Chemical Society

# Fumaric acid monoethyl ester-functionalized poly(D,L-lactide)/N-vinyl-2-pyrrolidone resins for the preparation of tissue engineering scaffolds by stereolithography

*Janine Jansen<sup>1</sup>, Ferry P.W. Melchels<sup>1</sup>, Dirk W. Grijpma<sup>1,2,\*</sup>, Jan Feijen<sup>1</sup>*

1) Institute for Biomedical Technology (BMTI) and Department of Polymer Chemistry and Biomaterials, Faculty of Science and Technology, University of Twente, P.O. Box 217, 7500 AE, Enschede, The Netherlands

2) Department of Biomedical Engineering, University Medical Center Groningen and University of Groningen, P.O. Box 196, 9700 AD Groningen, The Netherlands

\*D.W. Grijpma:

Corresponding author: Tel: +31-53-4892966; Fax: +31-53-4892155

E-mail: [d.w.grijpma@utwente.nl](mailto:d.w.grijpma@utwente.nl).

**RECEIVED DATE**

**ABSTRACT** Polymer networks were prepared by photo-crosslinking fumaric acid monoethyl ester (FAME) functionalized, three-armed poly(D,L-lactide) oligomers using N-vinyl-2-pyrrolidone (NVP) as diluent and comonomer. The use of NVP together with FAME-functionalized oligomers resulted in copolymerization at high rates, and networks with gel contents in excess of 90% were obtained. The hydrophilicity of the poly(D,L-lactide) networks increases with increasing amounts of NVP, networks containing 50 wt% of NVP absorbed 40% of water. As the amount of NVP was increased from 30 to 50 wt%, the Young's modulus after equilibration in water decreased from 0.8 to 0.2 GPa, as opposed to an increase from 1.5 to 2.1 GPa in the dry state. Mouse preosteoblasts readily adhered and spread onto all prepared networks. Using stereolithography, porous structures with a well-defined gyroid architecture were prepared from these novel materials. This allows the preparation of tissue engineering scaffolds with optimized pore architecture and tunable material properties.

**KEYWORDS** stereolithography, tissue engineering scaffolds, poly(D,L-lactide) macromers, fumaric acid monoethyl ester, N-vinyl-2-pyrrolidone, photo-polymerization, polymer networks, hydrophilicity

## Introduction

Stereolithography is a versatile solid free-form fabrication technique that can be applied to fabricate tissue engineering scaffolds<sup>1,2</sup>. It is based on spatially controlled photo-polymerization of a liquid resin. As the resin only solidifies where illuminated, a specific pattern can be created in one single layer. By repeating this process, three-dimensional structures can be built in a layer-by-layer manner. Unlike most other solid free-form fabrication techniques, stereolithography allows the manufacturing of nearly any designed 3D geometry. This enables the preparation of tissue engineering scaffolds with most favorable architectures for cell seeding and culturing. Besides this, stereolithography facilitates personalized tissue engineering scaffolds based on medical imaging data.

Commercially available materials for use in stereolithography are epoxy- or acrylate-based resins that give networks that often are neither biocompatible nor biodegradable. In biomedical applications, the ideal resin material should not only show fast photo-crosslinking kinetics, but should also promote cell adhesion and growth, and have suitable mechanical properties after crosslinking. Different resins that have been proposed are based on poly(propylene fumarate) (PPF)<sup>3,4</sup>, trimethylene carbonate (TMC) (co)polymers<sup>5-8</sup> and poly(ethylene glycol) (PEG)<sup>9,10</sup>.

Lactide polymers are well-known polymers that have been applied successfully in medical applications such as resorbable bone fixation devices<sup>11</sup> and in the preparation of tissue engineering scaffolds<sup>1</sup>. To allow polylactide network formation by photo-crosslinking, double bond-containing lactide oligomers are required. Fumaric acid derivatives are attractive compounds for end-functionalization, since fumaric acid is naturally found in the body. However, compared to the frequently used (meth)acrylate-functionalized oligomers, the reactivity of fumarate-functionalized oligomers is much lower. This can be overcome by choosing a suitable comonomer in the crosslinking reaction. N-vinyl-2-pyrrolidone (NVP) is a monomer that can copolymerize with fumaric acid derivatives at high rates<sup>12,13</sup>, and poly(N-vinyl-2-pyrrolidone) (PVP) is a hydrophilic biocompatible polymer that is used as an additive in pharmaceuticals<sup>14</sup>. Using the Q-e scheme<sup>15,16</sup>, the calculated copolymerization constants for diethyl fumarate and NVP are,

respectively, 0.0004 and 0.0007. This implies that alternating copolymers will form when fumaric acid derivatives and NVP are copolymerized. As a result of the strong polar interactions between diethyl fumarate and NVP, rapid polymerization of diethyl fumarate derivatives is also to be expected. In stereolithography, high photo-polymerization and crosslinking rates are required.

In this paper we describe the preparation and characterization of photo-crosslinked networks based on fumaric acid monoethyl ester (FAME) end-functionalized poly(D,L-lactide) (PDLLA) oligomers and N-vinyl-2-pyrrolidone. The influence of the amount of hydrophilic component on the properties of the resulting networks was studied. Liquid mixtures of three-armed (PDLLA 3-FAME) macromers and NVP as a reactive diluent were photo-polymerized.

One PDLLA 3-FAME/NVP resin was applied in stereolithography to prepare pre-designed biodegradable tissue engineering scaffolds.

## **Experimental**

### *Materials*

D,L-lactide was purchased from Purac Biochem (The Netherlands). Tin 2-ethylhexanoate ( $\text{Sn}(\text{Oct})_2$ ), glycerol, fumaric acid monoethyl ester (FAME), hematoxyline and paraformaldehyde were obtained from Sigma Aldrich (USA). 4-Dimethylaminopyridine (DMAP) was obtained from Merck (Germany). 1,3-Dicyclohexylcarbodiimide (DCC), triethyl amine (TEA) and N-vinyl-2-pyrrolidone (NVP), were purchased from Fluka (Switzerland). Irgacure 2959 (2-hydroxy-1-[4-(2-hydroxyethoxy)phenyl]-2-methyl-1-propanone) and Orasol Orange G, an orange dye soluble in organic solvents, were obtained from Ciba Specialty Chemicals (Switzerland). Lucirin TPO-L (ethyl 2,4,6-trimethylbenzoylphenyl phosphinate) was obtained from BASF (Germany). Alpha-MEM (minimum essential medium), and trypsin were purchased from Invitrogen (USA). L-glutamine, and fetal bovine serum (FBS) were purchased from Lonza (Switzerland). Phosphate-buffered saline (PBS) was obtained from B. Braun (Germany). Analytical grade dichloromethane (DCM from Biosolve, The Netherlands) was dried over

CaH<sub>2</sub> and distilled. All other solvents were of technical grade and were used as received from Biosolve (The Netherlands).

*Synthesis of star-shaped FAME-functionalized PDLLA oligomers*

Functionalized star-shaped oligomers (PDLLA 3-FAME macromers) were prepared by esterification of PDLLA oligomeric triols with FAME in the presence of DCC as a coupling agent and DMAP as a catalyst at room temperature (Figure 1)<sup>17, 18</sup>.

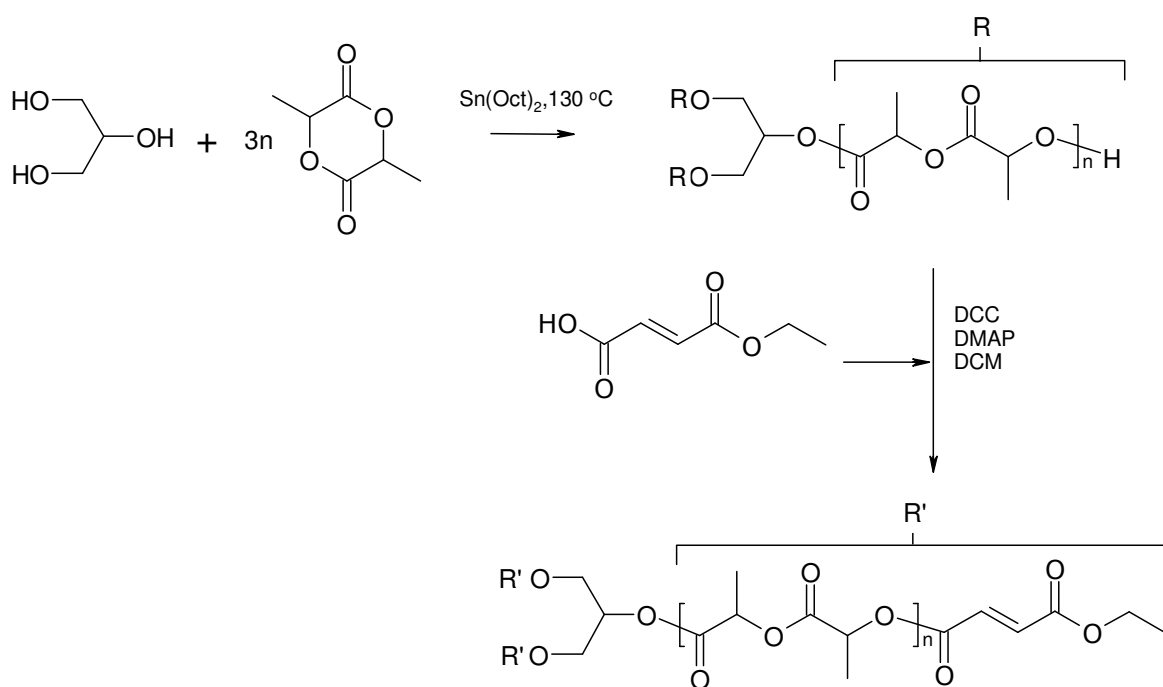


Figure 1. Scheme of the synthesis of FAME-functionalized PDLLA oligomers.

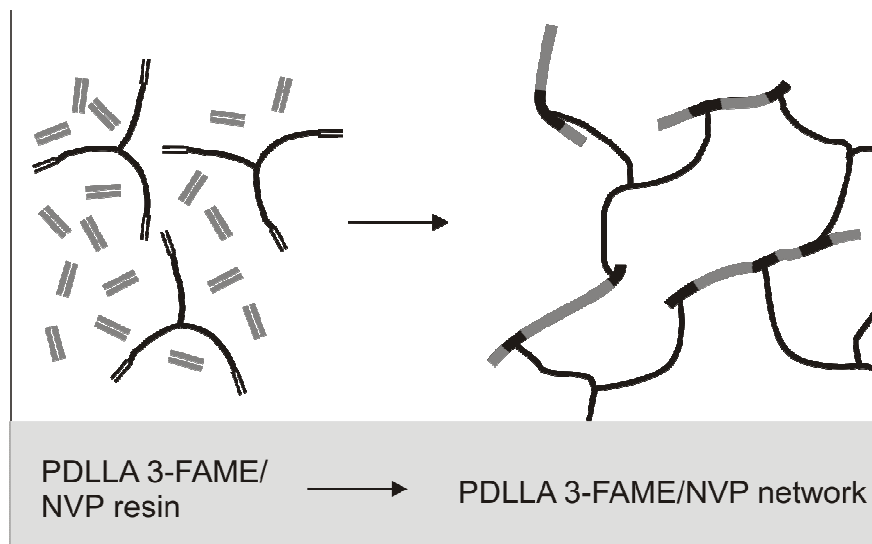
Batches (of 200 g and 175 g) of PDLLA oligomers were synthesized by ring opening polymerization of D,L-lactide in the presence of glycerol, a trifunctional initiator. D,L-lactide, glycerol and Sn(Oct)<sub>2</sub> as a catalyst were reacted in the melt at 130 °C for 24-48 h under argon. The targeted molecular weight was 3100 g/mol, which corresponds to approximately 7 lactide units per arm.

Amounts of oligomer (10-100 g) were charged into a three-necked flask, dried for 2 h at 110 °C in vacuo, and cooled to room temperature under argon. The oligomer was dissolved in dry DCM and, after addition and dissolution of FAME, further cooled to 0 °C . Then a dichloromethane solution of DCC and DMAP was added dropwise to the vigorously stirred oligomer solution. In the coupling reaction, 1.2 moles of FAME and DCC and 0.03 moles of DMAP per mole of hydroxyl groups were used. The reaction was continued overnight, letting the contents warm up slowly to room temperature. After completion of the reaction, the formed dicyclohexylurea was removed by filtration and the macromer was purified by precipitation in isopropanol, washing with water and freeze-drying.

High molecular weight (high MW) PDLLA ( $M_n = 4.7 \times 10^5$  g/mol,  $M_w = 6.3 \times 10^5$  g/mol, determined by gel permeation chromatography using a Viscotek GPC system equipped with a TDA 302 Triple Detector Array) was synthesized by ring opening polymerization of D,L-lactide at 130 °C using  $\text{Sn}(\text{Oct})_2$  as a catalyst and used as a reference material.

#### *Photo-crosslinking of PDLLA 3-FAME macromers and NVP*

Solutions containing macromer (50-80 wt%), NVP (20-50 wt%) and Irgacure 2959 photo-initiator (2 mole % per mole of macromer double bonds) were prepared. Photo-crosslinking was carried out by exposing specimens cast from these solutions to long-wave UV light (Ultralum crosslinking cabinet, wavelength 365 nm) for 15 min at a distance of 15 cm in a nitrogen atmosphere. The light intensity was 3-5 mW/cm<sup>2</sup>. Upon irradiation, the initiator molecules dissociate into radicals which initiate the addition copolymerization of FAME-end-groups and NVP diluent. A crosslinked network is thereby formed (Figure 2). After crosslinking, the samples were extracted with acetone in a Soxhlet apparatus for 1 d and dried under a nitrogen flow at 90 °C overnight and then at 120 °C for a few more hours.





$$\text{Gel content} = m_1/m_0 \times 100\%$$

For water uptake measurements, specimens of extracted networks ( $n = 3$ ) were weighed ( $m_d$ ) and equilibrated in distilled water for 1 d. The samples were removed from the water, blotted dry, and weighed again ( $m_s$ ). The water uptake was calculated using:

$$\text{Water uptake} = (m_s - m_d)/m_d \times 100\%$$

Contact angle measurements were carried out using an OCA 20 contact angle system from Dataphysics. Measurements were performed at room temperature on samples equilibrated in MilliQ water for 1 d using the captive air bubble method. Four measurements were performed per material. The air bubble volume was 70  $\mu\text{l}$ .

For tensile testing, samples ( $n = 3$ ) with dimensions of approximately  $100 \times 5 \times 0.5 \text{ mm}^3$  were prepared by crosslinking macromer solutions containing 30 to 50 wt% NVP in a Teflon mold. Solutions containing 20 wt% NVP were found to be quite viscous, making it difficult to prepare specimens that were free of air bubbles. The high molecular weight PDLLA samples that were used as a reference were prepared by compression molding at 140 °C using stainless steel molds. The maximal tensile strength, Young's modulus and elongation at break for the polymer networks were determined at room temperature using a Zwick Z020 tensile tester operated at a cross-head speed of 50 mm/min and an initial grip-to-grip separation of 50 mm. The deformation was determined from the grip-to-grip separation and therefore the calculated Young's modulus values are only an indication of the stiffness of the networks.

### *Cell adhesion*

Mouse preosteoblasts, from the MC3T3 cell line (ATCC number = CRL-2593) were cultured in T75 cell culture flasks in  $\alpha$ -MEM medium supplemented with 2 mM L-glutamine and 10 % FBS. The cells were cultured for 2 d at 37 °C in a 5 % CO<sub>2</sub> atmosphere, trypsinized at 37 °C for about 5 min, and redispersed in medium. The concentration of cells was adjusted to 200,000 cells/ml.

Disk-shaped network samples ( $\varnothing = 12$  mm) were prepared in a Teflon mold, while high molecular weight PDLA samples were prepared by compression molding (140 °C). From these compression molded samples, 12 mm diameter disks were cut out with a hollow punch. Of all materials, 3 samples were disinfected in isopropanol (2x15 min), washed with PBS (2x15 min) and placed in ultra-low cell binding 24-well plates. An amount of 500  $\mu$ l of cell suspension, containing 100,000 cells, was then pipetted onto each sample. As a control, tissue culture polystyrene (TCPS) was seeded at the same density as the PDLA 3-FAME/NVP networks and PDLA samples. The cell-seeded disks were kept at 37 °C under 5 % CO<sub>2</sub> for 6 h.

After this time period, culture medium and unattached cells were removed by rinsing the materials twice with PBS. The remaining cells were then fixed with formalin (4 % formaldehyde) for 15 min and subsequently washed with PBS. The samples were stained with hematoxylin and washed twice with distilled water. Cell adhesion to the different substrates was examined using an inverted light microscope.

### *Stereolithography*

The viscosities of the PDLA 3-FAME/NVP solutions were determined using a Brookfield DV-E viscometer equipped with a small sample adapter. For different macromer concentrations, the viscosity at 10 rpm (corresponding to a shear rate of 0.93 s<sup>-1</sup>) was determined at 25 °C.

To a solution containing 65 wt% PDLA 3-FAME and 35 wt% NVP, 5 wt% of Lucirin TPO-L photo-initiator and 0.5 wt% Orasol Orange G dye (both relative to the amount of macromer) were added. This resin was used to prepare porous structures by stereolithography with a commercially available set-up

(Perfactory Mini Multilens, EnvisionTec). This stereolithography apparatus makes use of blue light of a wavelength of 400-550 nm, with a peak at 440 nm. In this range of wavelengths, Lucirin TPO-L is suited to photo-initiate radical polymerization, while Orasol Orange G allows control of light penetration into the resin.

Porous gyroid structures<sup>19</sup>, with a porosity of 76 % were designed and built at a resolution of 16.5  $\mu\text{m}$  in the x- and y-directions, the layer thickness (and the resolution in the z-direction) was 15  $\mu\text{m}$ . The curing time per layer was 8 s at a light intensity of 20  $\text{mW}/\text{cm}^2$ .

### *Scaffold characterization*

Scanning electron microscopy (SEM) (Philips XL30 operated at 5 kV) and micro-computed tomography ( $\mu\text{CT}$ ) (GE eXplore Locus SP  $\mu\text{CT}$  scanner, the spatial resolution applied was 8  $\mu\text{m}$ ) were used to visualize and to characterize the built scaffolds. The grayscale image obtained from the  $\mu\text{CT}$  scan was thresholded to distinguish between polymer voxels and pore voxels (voxels being 8 x 8 x 8  $\mu\text{m}^3$  volume-elements).

The porosity was calculated as the fraction of pore voxels within the scaffold. To determine pore size, pores are entirely filled with as large as possible (overlapping) spheres<sup>20</sup>. To every pore voxel, a pore size that corresponds to the diameter of the largest sphere that contains that voxel is then assigned. From the distribution of pore sizes, a volume-averaged pore size can be calculated. The accessible pore volume is determined as the volume of the scaffold that can be reached from the exterior by simulating the percolation of a spherical particle through the interconnected pore network<sup>21</sup>. This was done for a range of diameters of 8 to 400  $\mu\text{m}$ . The specific surface area was calculated as the sum of the areas of the boundaries between pore voxels and polymer voxels.

## **Results and discussion**

### Synthesis of star-shaped, FAME-functionalized PDLLA oligomers

Using glycerol as a trifunctional initiator, D,L-lactide was polymerized by ring opening polymerization to yield three-armed oligomers. The number average molecular weights of the prepared batches were  $3.1 \times 10^3$  and  $3.2 \times 10^3$  g/mol as determined from the glycerol to lactide ratio in NMR spectra.

The coupling of fumaric acid monoethyl ester (FAME) to PDLLA oligomers to form PDLLA 3-FAME was confirmed by appearance of a  $-\text{CH}=\text{CH}-$  (e) peak at  $\delta$  6.90, of  $-\text{CH}_2-$  (f) peaks at  $\delta$  4.28 and of  $-\text{CH}_3$  (g) peaks at  $\delta$  1.32 in the NMR spectra of PDLLA 3-FAME, as shown in Figure 3. Based on the relative intensities of peaks (e) and (a), the calculated degrees of functionalization varied between 86 and 97 %. When calculating the degrees of functionalization from peaks (a) and (g), values between 99% and 100% were obtained.

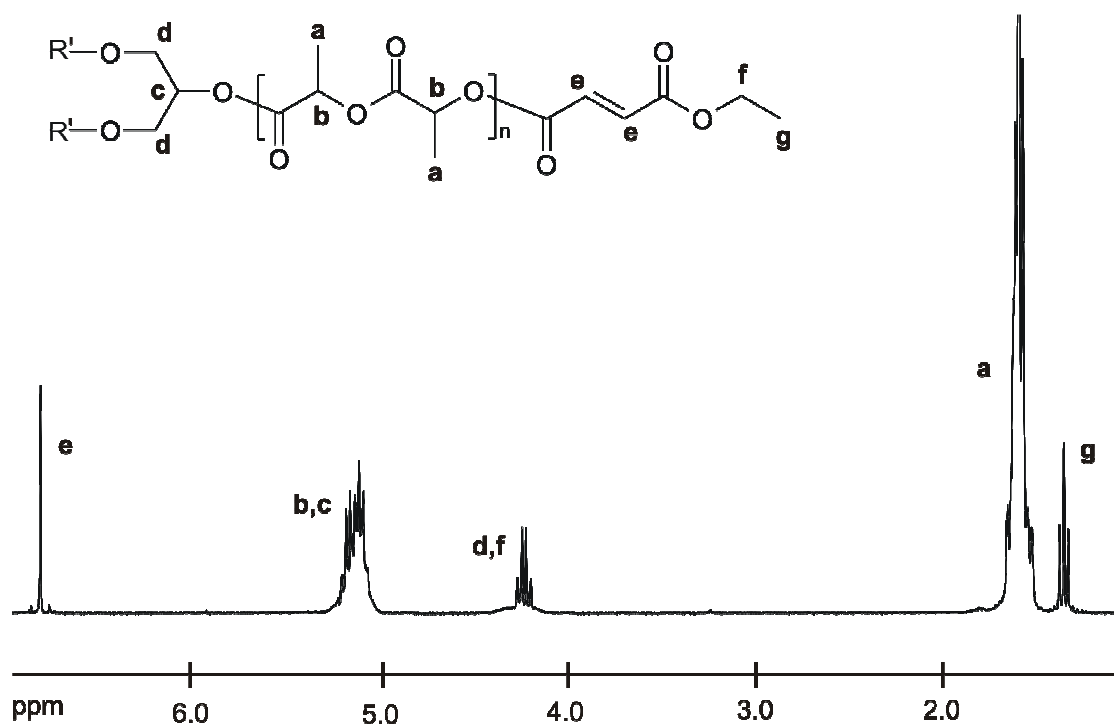


Figure 3. Example of a  $^1\text{H}$ -NMR spectrum of PDLLA 3-FAME.

### Photo-crosslinking of PDLLA 3-FAME macromers and NVP

Networks were formed from PDLLA 3-FAME macromers and NVP by UV irradiation (365 nm) using Irgacure 2959 as a biocompatible initiator<sup>22, 23</sup>. The NVP content was varied from 20 to 50 wt%, as only compositions containing more than 20 wt% NVP are liquid at room temperature.

The influence of NVP content on the network properties was evaluated. The gel content of the networks obtained after a polymerization time of only 15 min was above 90 % in all cases (Table 1). When similar 3-FAME macromers were crosslinked under comparable conditions in the absence of NVP, a long irradiation time of 3 h was required to reach a gel content of 81 %<sup>17</sup>. The addition of NVP as a comonomer clearly results in a significant increase in crosslinking rates. This will enable application of PDLLA 3-FAME macromers in stereolithography.

The glass transition temperatures of the oligomers, macromers and extracted networks in the dry state were determined by DSC and are presented in Table 1. It can be seen that upon network formation, the glass transition temperature increases. The NVP-containing networks have  $T_g$  values that are significantly higher than that of high MW PDLLA. With higher NVP contents,  $T_g$  of the networks increases as expected. All networks showed a single glass transition, which indicates that NVP was homogeneously incorporated into the network structure.

Table 1. Gel contents and glass transition temperatures of networks prepared from PDLLA 3-FAME macromers and NVP.  $T_g$  values of PDLLA oligomers, high MW PDLLA and high MW PVP are given as a reference.

	NVP content (wt%)	Gel content (%)	$T_g$ (°C)
PDLLA oligomer	0	-	31.1
PDLLA 3-FAME macromer	0	-	38.1
PDLLA 3-FAME network <sup>a)</sup>	0	81.4	38.6
PDLLA 3-FAME/NVP network	20	93.5 ± 1.8	66.8
PDLLA 3-FAME/NVP network	30	93.3 ± 0.3	81.4
PDLLA 3-FAME/NVP network	40	92.7 ± 0.2	85.3
PDLLA 3-FAME/NVP network	50	90.9 ± 0.6	95.6
high MW PDLLA	0	-	55.1
high MW PVP <sup>b)</sup>	100	-	179

a) Data from reference 18. Non-extracted networks, prepared from macromers with  $M_n = 4750$  g/mol. The macromer films were cast from chloroform and irradiated at 365 nm for 3 hrs.

b) Data from reference 15.  $M_w = 9 \times 10^5$  g/mol.

PDLLA 3-FAME networks containing NVP absorb significantly more water than high molecular weight PDLLA (Figure 4). Due to the hydrophilic character of NVP, the water uptake of the networks increases with increasing NVP content. The hydrophilicity of the resulting networks can readily be adjusted and materials ranging from hydrophobic glassy polymer networks to hydrogels can be prepared.

Networks containing NVP had a lower contact angle than high MW PDLLA. The contact angle of the networks is comparable to that of tissue culture polystyrene (TCPS). As a result of poor wetting cell seeding into porous PLA scaffolds can be problematic <sup>24</sup>. It can be expected that the increased

hydrophilicity of PDLLA 3-FAME/NVP will facilitate cell seeding into porous scaffolds prepared from these networks. The water uptake of the networks showed a much stronger dependence on the NVP content than the contact angle. When increasing the NVP content in the networks from 20 % to 50%, the contact angles remain essentially constant. Apparently, the concentration of hydrophilic components at the surface of the specimens is similar. This may be caused by reorganization of the PVP-containing copolymer chains.

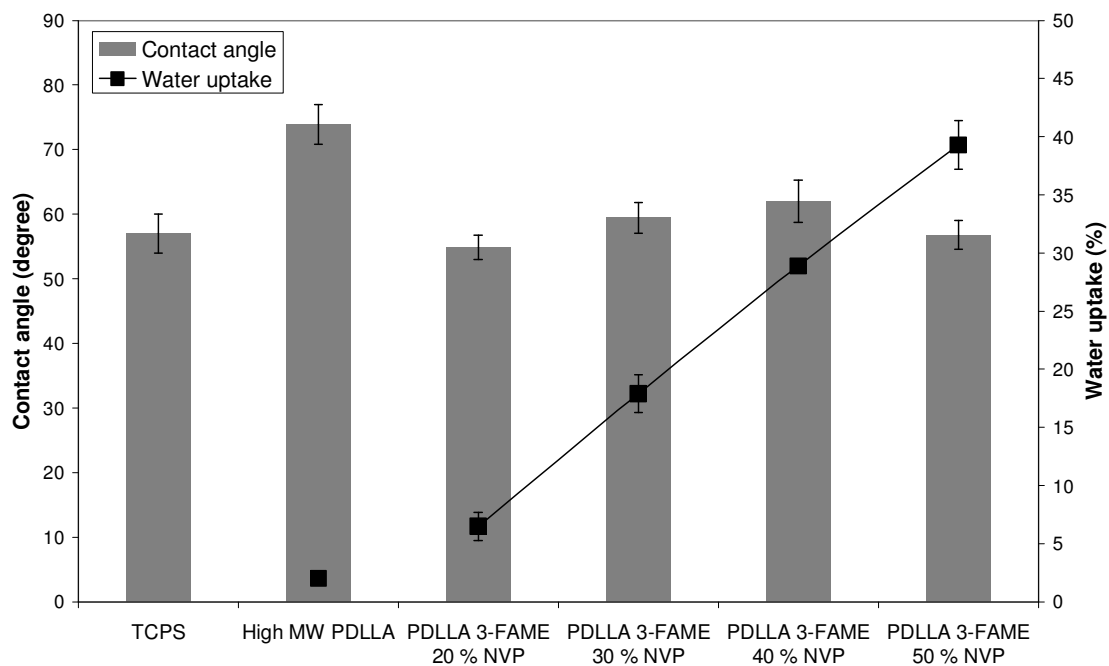


Figure 4. Contact angles (bars) and water uptake (■) of PDLLA 3-FAME/NVP networks conditioned in water at 37 °C for 2 days. Reference values for TCPS and high MW PDLLA are given as well.

During cell seeding and culturing, and upon implantation in the human body, tissue engineering scaffolds can take up significant amounts of water. To investigate the effect of water uptake on the mechanical properties of PDLLA 3-FAME/NVP networks, specimens were analyzed in the dry state and after equilibration in water. Their tensile properties are given in Table 2.

Table 2. Tensile properties of PDLLA 3-FAME/NVP networks in the dry state and after equilibration in water.

	NVP content (wt%)	Dry/Wet	Young's modulus (GPa) <sup>a)</sup>	Tensile strength (MPa)	Elongation at break (%)
PDLLA 3-FAME network <sup>b)</sup>	0	dry	0.01	1.3	106
High MW PDLLA	0	dry	1.6 ± 0.1	48 ± 1	4.5 ± 0.2
PDLLA 3-FAME/NVP network	30	dry	1.5 ± 0.1	42 ± 4	3.1 ± 0.3
PDLLA 3-FAME/NVP network	40	dry	1.8 ± 0.1	34 ± 10	2.2 ± 0.8
PDLLA 3-FAME/NVP network	50	dry	2.1 ± 0.1	56 ± 10	3.4 ± 0.9
High MW PDLLA <sup>c)</sup>	0	wet	1.5	42	2.9
PDLLA 3-FAME/NVP network	30	wet	0.8 ± 0.1	20 ± 3	3.0 ± 0.7
PDLLA 3-FAME/NVP network	40	wet	0.8 ± 0.1	19 ± 1	3.9 ± 0.2
PDLLA 3-FAME/NVP network	50	wet	0.2 ± 0.0	7 ± 1	7.3 ± 1.8

a) The deformation was determined from the grip-to-grip separation, therefore the given Young's modulus values are only an indication of the stiffness of the networks.

b) Data from reference 18. Non-extracted networks, prepared from macromers with  $M_n = 4750$  g/mol. The macromer films were cast from chloroform and irradiated at 365 nm for 3 hrs.

c) Single measurement.

In the dry state, the Young's modulus of the networks increased with increasing NVP content. In the wet state this trend is reversed, as networks with higher NVP contents absorb larger amounts of water. High molecular weight PDLLA absorbed only 2 wt% of water, and showed the smallest difference in Young's modulus values between the dry and wet states. PDLLA 3-FAME networks containing 50 % NVP absorbed 40 % of water, and showed the lowest modulus upon conditioning. A scaffold material with suitable properties for a specific tissue can be synthesized by adjusting NVP content. The tensile strength of dry networks does not significantly change with NVP content. In the wet state however,



tensile strengths of the networks decrease significantly with increasing NVP contents. No major differences in the elongation at break as a function of NVP content were observed.

When compared to PDLLA 3-FAME networks prepared previously in our group without a reactive diluent<sup>17</sup>, these NVP-containing networks show much higher Young's modulus and tensile strength values. Although, this can partly be explained by the presence of a sol fraction and chloroform remaining in the non-extracted networks described in our earlier work, the number of elastically inactive chains in the network is significantly reduced upon copolymerization of the PDLLA macromer with NVP. This results in networks with much better mechanical properties.

#### *Cell adhesion to PDLLA 3-FAME/NVP networks*

To assess the suitability of these networks for cell culturing and tissue engineering, initial cell adhesion experiments were performed. Representative micrographs of the surfaces of different PDLLA 3-FAME/NVP and reference materials six hrs after cell seeding are shown in Figure 5. It can be observed that the MC3T3 cells adhered well to the copolymer networks, showing a spread morphology. This is indicative of interactions of cell membrane integrins with surface-adsorbed proteins, facilitating subsequent cell spreading. The behavior of the cells on the network films is comparable to that on the high molecular weight PDLLA and TCPS controls. Even though it seems that the cells had a slightly higher tendency to aggregate on the networks with the highest NVP contents, the results indicate good cell adhesion for the range of PDLLA 3-FAME/NVP networks investigated. Although surface hydrophilicity is only one parameter that influences cell adhesion, the observed cell adhesion is consistent with the similarity of the contact angles. For all the NVP-containing networks, the contact angles are comparable to each other and to TCPS (Figure 4). Thus, by adjusting the NVP content, water uptake and mechanical properties of these photo-crosslinked PDLLA 3-FAME/NVP networks can be tailored without consequences for their cell adhesion properties.

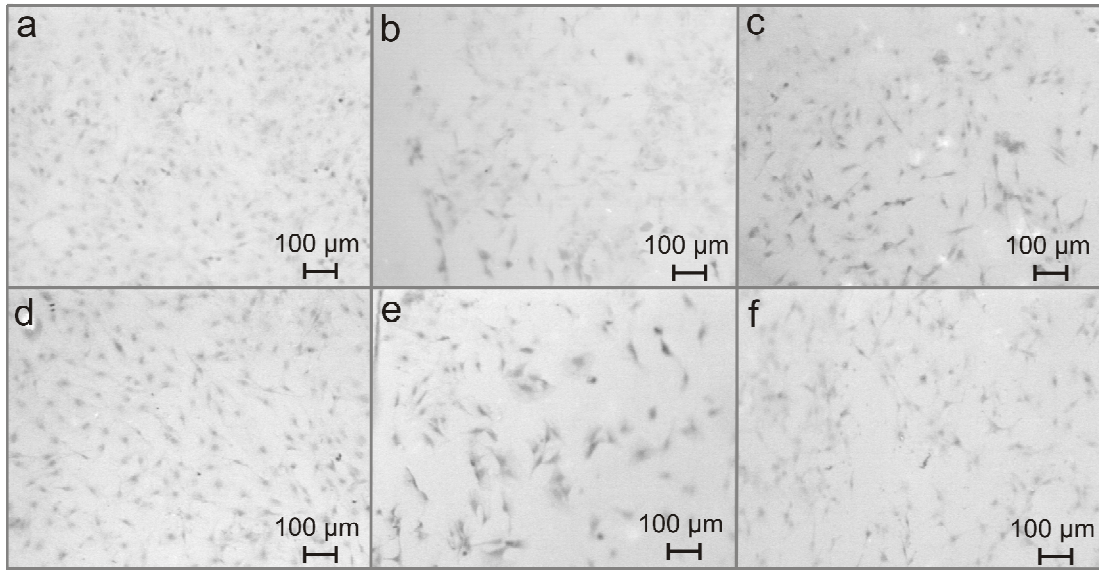


Figure 5. Light microscopy images of the adhesion of MC3T3 cells after 6 hrs to (a) TCPS, (b) high MW PDLLA, (c) PDLLA 3-FAME/20 % NVP network, (d) PDLLA 3-FAME/30 % NVP network, (e) PDLLA 3-FAME/40 % NVP network and (f) PDLLA 3-FAME/50 % NVP network.

### *Stereolithography*

The favorable mechanical and biological properties of the prepared networks encourage their application in tissue engineering. Therefore, we investigated the possibility of preparing porous structures from PDLLA 3-FAME macromers and NVP formulations by stereolithography.

Besides a high curing rate upon irradiation, a suitable viscosity of the resin is important to allow processing by stereolithography. The viscosities of resins that are applied in stereolithography range from 250 cP for a pentaerythritol tetra-acrylate resin to 5000 cP for ceramic suspensions<sup>25</sup>. The viscosity of PDLLA 3-FAME/NVP resins could easily be adjusted by variation of the amount of reactive NVP diluent. As the NVP content was increased from 35 to 45 wt %, the viscosity of the resin at 25 °C and a shear rate of  $9.3 \text{ s}^{-1}$  decreased from  $4.1 \times 10^3$  to  $0.7 \times 10^3$  cP. These resin viscosities are suitable for application in stereolithography.

To build porous tissue engineering scaffolds in a stereolithography setup, a mixture of PDLLA 3-FAME, 35 wt% NVP, 5 wt% (relative to the amount of macromer) Lucirin photo-initiator and 0.5 wt%

(relative to the amount of macromer) Orasol Orange G dye was prepared. The three dimensional design that was chosen for the scaffolds was a gyroid. Structures built according to this mathematically defined architecture, have a large specific surface area and high pore interconnectivity. These characteristics make it an excellent architecture for tissue engineering, as it enables cell-seeding at high densities, and allows homogeneous distribution of cells and flow of nutrients throughout the scaffold.

In the design we used, the porosity and pore size (*i.e.* the diameter of the open channels running through the structure) were 76 % and 260  $\mu\text{m}$ , respectively.

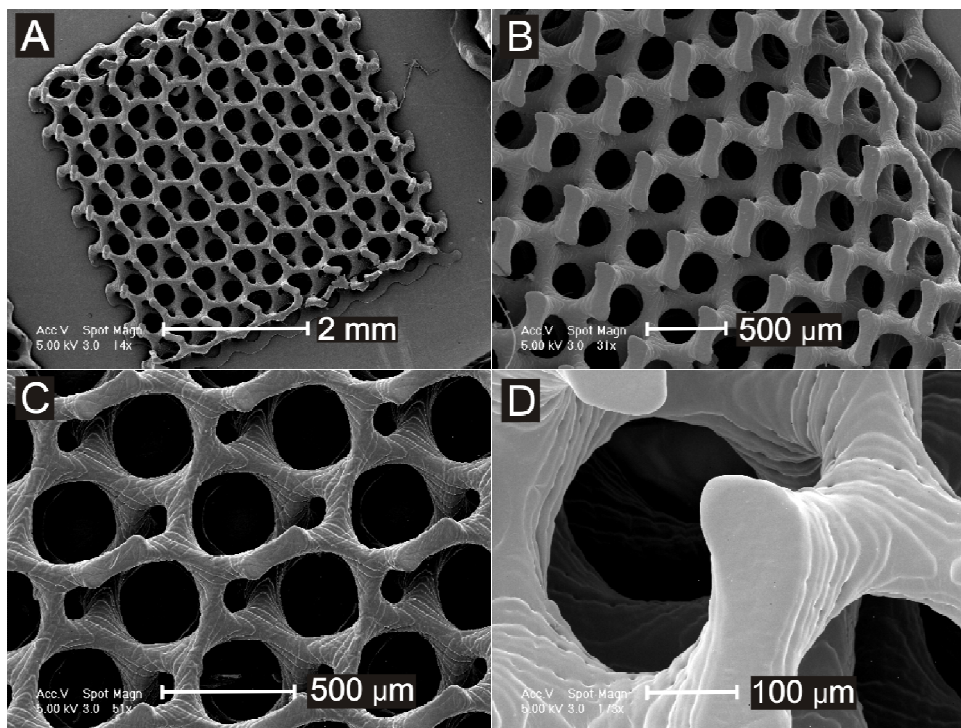


Figure 6. SEM images of porous PDLLA 3-FAME/NVP gyroid structures built by stereolithography.

Figure 6 shows SEM images of a built porous gyroid structure. It follows that use of the PDLLA 3-FAME/NVP resin in stereolithography enables the preparation of biodegradable scaffolds with highly controlled architectures. The built scaffolds measured approximately 4.5 x 4.5 x 1.8 mm and closely

resembled the design. It can be seen that the pore network is homogenous in size and fully interconnected. At higher magnifications, the layer-by-layer nature of the construct is clearly visible.

The occurrence of polymerization shrinkage can be seen at the edges of the construct in Figure 6 B. This has resulted in a size reduction of 16 %; the width of the top part of the structure is 4.2 mm, while the designed structure was 5 mm wide. The top part of the scaffold has shrunk more than the lower part, and some fractures can be observed as well (Figure 6 A). By incorporating a support structure into the design (which has not yet been done here), the effects of polymerization shrinkage in stereolithography can be dealt with.

Figure 7 depicts a  $\mu$ CT-visualization of part of an equivalent scaffold built using the PDLA 3-FAME/NVP resin. It is apparent that the prepared structure is highly regular in all three dimensions. The  $\mu$ CT data can also be used to quantify relevant scaffold parameters.

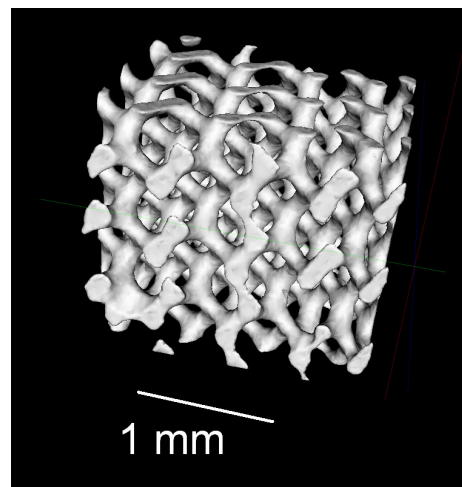


Figure 7.  $\mu$ CT-visualization of part of a porous gyroid structure built using PDLA 3-FAME/NVP.

A porosity of 80 % and an average pore size of 256  $\mu$ m were determined. The values for porosity and pore size match those of the design closely. The deviations are less than 5 % and can be the result of inaccuracies in the digitalization procedure during the creation of the build file, in the polymerization

process, in the imaging, in the three-dimensional reconstruction of the scanning data or in the method of assigning sizes to pores.

Figure 8 shows the pore size distribution of the built gyroid structure as determined by  $\mu$ CT according to the described algorithm. Pores ranging in size from 240 to 350  $\mu\text{m}$  make up more than 80 % of the pore volume. The pore sizes smaller than 240  $\mu\text{m}$  are an inevitable artefact of the employed assignment algorithm, which assumes a spherical pore geometry. As a result, pore voxels that do not lie in the largest sphere that fits in a non-spherical pore, are assigned a too small pore size<sup>21</sup>.

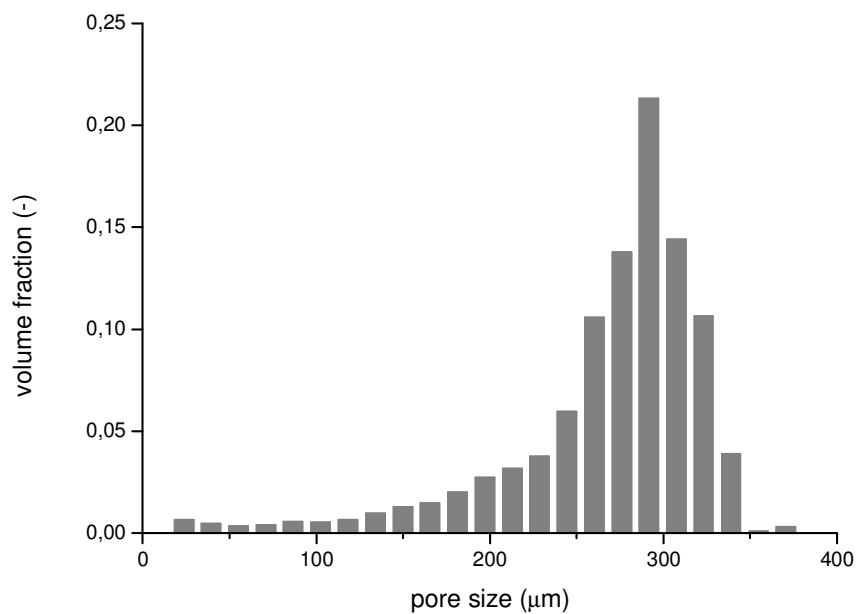


Figure 8: Pore size distribution of the porous gyroid structure shown in Figure 7 determined from  $\mu$ CT-data.

The interconnectivity of the pore structure of a scaffold can be quantified by assessment of its accessible pore volume, as is done in Figure 9. The accessible pore volume is the volume that can be reached from the outside of the imaged scaffold by simulating the permeation of a spherical particle. The figure shows that more than 90 % of the pore volume in this gyroid structure is connected to the outside

by channels with diameters larger than 100  $\mu\text{m}$ . This indicates high permeability of the scaffold for cells in a cell seeding procedure, and for nutrients and metabolites during cell culture or implantation.

From the  $\mu\text{CT}$ -data, a high specific surface area of 34  $\text{mm}^2$  per  $\text{mm}^3$  of scaffold could also be calculated. This large surface area and high porosity allows large numbers of cells to adhere, to proliferate and to deposit extra-cellular matrix.

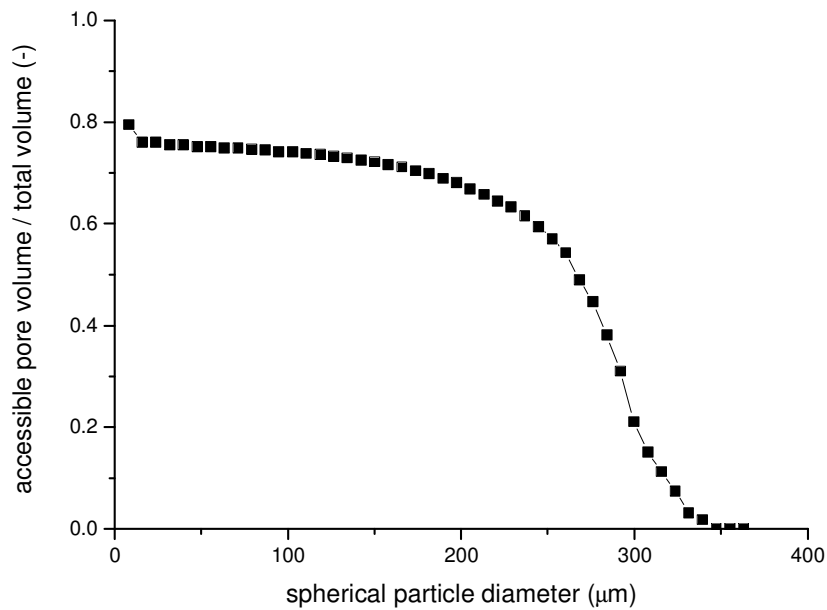


Figure 9: The accessible pore volume for simulated permeating spherical particles of different diameters. (The initial step-wise decrease in accessible pore volume from 8 to 16  $\mu\text{m}$  is a result of the limited resolution which leads to surface roughness). The data applies to the gyroid structure presented in Figure 7.

Since these materials show good cell adhesion and the architecture of the prepared scaffolds is optimal for cell seeding and culturing, these structures are most suited as tissue engineering scaffolds.

Currently the degradation behavior, long-term cell culturing and *in vivo* application of these PDLLA 3-FAME/NVP materials and scaffolds prepared by stereolithography are being investigated.

## Conclusions

Copolymerization of FAME-functionalized PDLLA macromers with NVP as a reactive diluent resulted in the rapid formation of networks with high gel contents. By varying the amount of NVP, the material properties of the networks (such as water uptake and rigidity) can be tailored. Mouse preosteoblast cells adhered and spread well onto all materials, NVP content did not have a significant effect.

Using stereolithography, a porous gyroid structure was prepared at high resolution from a PDLLA 3-FAME/NVP resin. This scaffold design was chosen for its favorable open and interconnected pore architecture. The obtained structure very closely resembled the computer-aided design.

These resins may find wide application in stereolithography and tissue engineering.

## Acknowledgements

We would like to acknowledge R. Gabbrielli and C.R. Bowen (University of Bath, UK) for providing the gyroid CAD-file and the EU for funding (STEPS project, FP6-500465).

## Supporting Information Available

DSC curves of PDLLA oligomers, PDLLA 3-FAME macromers and PDLLA 3-FAME/NVP networks are supplied as supporting information. This information is available free of charge via the Internet at <http://pubs.acs.org>.

## References

1. Hutmacher, D. W., Scaffolds in tissue engineering bone and cartilage. *Biomaterials* **2000**, *21*, 2529-2543.
2. Hutmacher, D. W.; Sittinger, M.; Risbud, M. V., Scaffold-based tissue engineering: rationale for computer-aided design and solid free-form fabrication systems. *Trends in Biotechnology* **2004**, *22*, 354-362.

3. Cooke, M. N.; Fisher, J. P.; Dean, D.; Rinnac, C.; Mikos, A. G., Use of stereolithography to manufacture critical-sized 3D biodegradable scaffolds for bone ingrowth. *Journal of Biomedical Materials Research* **2003**, 64B, 65-69.
4. Lee, J. W.; Lan, P. X.; Kim, B.; Lim, G.; Cho, D.-W., 3D scaffold fabrication with PPF/DEF using micro-stereolithography. *Microelectronic Engineering* **2007**, 84, 1702-1705.
5. Kwon, I. K.; Matsuda, T., Photo-polymerized microarchitectural constructs prepared by microstereolithography (uSL) using liquid acrylate-end-capped trimethylene carbonate-based prepolymers. *Biomaterials* **2005**, 26, 1675-1684.
6. Lee, S.-J.; Kang, H.-W.; Park, J.; Rhie, J.-W.; Hahn, S.; Cho, D.-W., Application of microstereolithography in the development of three-dimensional cartilage regeneration scaffolds. *Biomedical Microdevices* **2008**, 10, 233-241.
7. Matsuda, T.; Mizutani, M., Liquid acrylate-endcapped biodegradable poly(e-caprolactone-co-trimethylene carbonate). II. Computer-aided stereolithographic microarchitectural surface photoconstructs. *Journal of Biomedical Materials Research* **2002**, 62, 395-403.
8. Mizutani, M.; Arnold, S. C.; Matsuda, T., Liquid, Phenylazide-End-Capped Copolymers of e-Caprolactone and Trimethylene Carbonate: Preparation, Photocuring Characteristics, and Surface Layering. *Biomacromolecules* **2002**, 3, 668-675.
9. Dhariwala, B.; Hunt, E.; Boland, T., Rapid Prototyping of Tissue-Engineering Constructs, Using Photopolymerizable Hydrogels and Stereolithography. *Tissue Engineering* **2004**, 10, 1316-1322.
10. Mapili, G.; Lu, Y.; Chen, S.; Roy, K., Laser-layered microfabrication of spatially patterned functionalized tissue-engineering scaffolds. *Journal of Biomedical Materials Research Part B: Applied Biomaterials* **2005**, 75B, 414-424.



11. Athanasiou, K. A.; Agrawal, C. M.; Barber, F. A.; Burkhart, S. S., Orthopaedic applications for PLA-PGA biodegradable polymers. *Arthroscopy-the Journal of Arthroscopic and Related Surgery* **1998**, 14, 726-737.
12. Sharifi, S.; Mirzadeh, H.; Imani, M.; Atai, M.; Ziaee, F., Photopolymerization and shrinkage kinetics of in situ crosslinkable N-vinyl-pyrrolidone/poly( $\epsilon$ -caprolactone fumarate) networks. *Journal of Biomedical Materials Research Part A* **2008**, 84A, 545-556.
13. Yaszemski, M. J.; Payne, R. G.; Hayes, W. C.; Langer, R.; Mikos, A. G., In vitro degradation of a poly(propylene fumarate)-based composite material. *Biomaterials* **1996**, 17, 2127-2130.
14. Ko, J. H., Poly(N-vinyl pyrrolidone). In *Polymer Data Handbook*, Oxford University Press, New York 1999; pp 962-964.
15. Brandrup, J.; Immergut, E. H.; Abe, A.; Bloch, D. R., *Polymer Handbook*. Wiley-Interscience New York, 1999.
16. Odian, G., *Principles of Polymerization*. 3 ed.; Wiley-Interscience New York, 1991.
17. Grijpma, D. W.; Hou, Q.; Feijen, J., Preparation of biodegradable networks by photo-crosslinking lactide,  $\epsilon$ -caprolactone and trimethylene carbonate-based oligomers functionalized with fumaric acid monoethyl ester. *Biomaterials* **2005**, 26, 2795-2802.
18. Hassner, A.; Alexanian, V., Direct room temperature esterification of carboxylic acids. *Tetrahedron Letters* **1978**, 19, 4475-4478.
19. Schoen, A. H., Infinite periodic minimal surfaces without self-intersections In Nasa Technical Note, NASA-TN-D-5541 1970.
20. Hildebrand, T.; Ruegsegger, P., A new method for the model-independent assessment of thickness in three-dimensional images. *Journal of Microscopy-Oxford* **1997**, 185, 67-75.
21. Claase, M. B.; de Bruijn, J. D.; Grijpma, D. W.; Feijen, J., Ectopic bone formation in cell-seeded poly(ethylene oxide)/poly(butylene terephthalate) copolymer scaffolds of varying porosity. *Journal of Materials Science-Materials in Medicine* **2007**, 18, 1299-1307.

22. Bryant, S. J.; Nuttelman, C. R.; Anseth, K. S., Cytocompatibility of UV and visible light photoinitiating systems on cultured NIH/3T3 fibroblasts in vitro. *Journal of Biomaterials Science, Polymer Edition* **2000**, 11, 439-457.
23. Williams, C. G.; Malik, A. N.; Kim, T. K.; Manson, P. N.; Elisseeff, J. H., Variable cytocompatibility of six cell lines with photoinitiators used for polymerizing hydrogels and cell encapsulation. *Biomaterials* **2005**, 26, 1211-1218.
24. Mikos, A. G.; Lyman, M. D.; Freed, L. E.; Langer, R., Wetting of poly(-lactic acid) and poly(-lactic-co-glycolic acid) foams for tissue culture. *Biomaterials* **1994**, 15, 55-58.
25. Hinczewski, C.; Corbel, S.; Chartier, T., Ceramic suspensions suitable for stereolithography. *Journal of the European Ceramic Society* **1998**, 18, 583-590.

